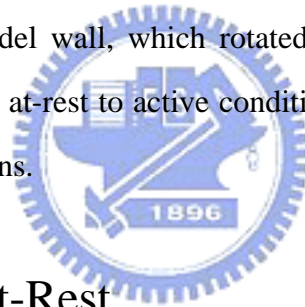


# Chapter 2

## LITERATURE REVIEW

Theories and experimental studies to estimate the lateral pressure acting on a retaining wall close to a rock face are summarized in this chapter. Theoretical and empirical relationship to estimate the lateral pressure of granular material acting on silos or storage bunkers were proposed by Janssen (1895), and Reimbert and Reimbert (1976). Spangler and Handy (1982) suggested theories to estimate the earth pressure near a rock face. Frydman and Keissar (1987) used the centrifuge modeling technique to test a small model wall, which rotated about its base, to observe the changes in pressures from the at-rest to active condition. Details of these theories are introduced in following sections.



### 2.1 Earth Pressure at-Rest

#### 2.1.1 Coefficient of Earth Pressure

Donath (1891) was the first to introduce the concept of “the stationary pressure of unlimited ground”. Donath defined the coefficient as the ratio of the effective horizontal pressure ( $\sigma_h$ ) to the effective vertical earth pressure ( $\sigma_v$ ) resulting in soil due to the application of vertical load.

$$K = \frac{\sigma_h}{\sigma_v} \quad (2.1)$$

#### 2.1.2 Coefficient of Earth Pressure at-Rest

The coefficient at-rest  $K_o$  is refer to the condition where no lateral yielding occurs, under the condition of constrained lateral deformation. As shown in Fig. 2.1(a), the overburden pressure  $\sigma_v$  compresses the soil element A formed in a horizontal sedimentary deposit. During the formation of the deposit, the element is consolidated under this vertical pressure. The vertical stress produces a lateral deformation against surrounding soils due to the Poisson's ratio effect. However, based on the definition and the field observation, over the geological period, the horizontal strain is kept to zero. It is concluded that the surrounding soil resists the lateral deformation with a developed lateral stress  $\sigma_h$ . A stable stress state will develop in which  $\sigma_h$  and  $\sigma_v$  become stresses acting on the vertical and horizontal planes as shown in Fig. 2.1(b). For an isotropic soil element shown in Fig. 2.2, if the soil behaved as an ideal elastic material, based on the mechanics of materials, the lateral strain  $\varepsilon_y$  can be expressed as:



$$\varepsilon_y = \frac{\sigma_y}{E} - \frac{\nu}{E}(\sigma_x + \sigma_z) \quad (2.2)$$

or

$$\varepsilon_h = \frac{\sigma_h}{E} - \frac{\nu}{E}(\sigma_h + \sigma_v) \quad (2.3)$$

where  $E$  is the elastic modulus and  $\nu$  is the Poisson's ratio of the soil.

Base on the definition of the at-rest condition, the lateral strain would be zero under the application of stress state and the  $\sigma_h = K_o \sigma_v$ . Then the Eq. 2.3 can be written as:

$$\varepsilon_h = \frac{1}{E}(K_o \sigma_v - \nu K_o \sigma_v - \nu \sigma_v) = 0 \quad (2.4)$$

and the coefficient of earth pressure at-rest  $K_o$ :

$$K_o = \frac{\nu}{1-\nu} \quad (2.5)$$

It should be mentioned that Eq. 2.5 is applicable for the isotropic and elastic materials only. However, the behavior of soil element is more complex and far from these assumptions. It is evident that the relationship between  $K_o$  and elastic parameter  $\nu$  of Eq. 2.5 is obsolescent for predicting in-situ horizontal stress.

### 2.1.3 Jaky's Formula

Attempts have been made to establish a theoretical relationship between the strength properties of a soil and  $K_o$ . The empirical relationship to estimate  $K_o$  of coarse-grained soil is discussed in this section.

Mesri and Hayat (1993) reported that Jaky (1944) arrived at a relationship between  $K_o$  and angle of internal friction  $\phi$  by analyzing a talus of granular soil freestanding at the angle of repose. Jaky (1944) assumed that the angle of repose is equal to the angle of internal friction  $\phi$ . This assumption is reasonable for sedimented, normally consolidated materials for which the angle of repose is equal to the constant-volume friction angle,  $\phi_{cv}$  (Cornforth, 1973). Darwin (1883) defined the angle of repose as the greatest inclination to the horizon at which a talus will stand. Jaky (1944) reasoned that the sand cone OAD in Fig. 2.3 is in a state of equilibrium and its surface and inner points are motionless. The horizontal pressure acting on OC is the earth pressure at-rest. Slide planes exist in the inclined sand mass. One set of these planes makes an angle  $\phi$  with the horizontal, and the second set of slide planes crosses the first one at an angle of  $(90^\circ - \phi)$ . However, as OC is a line of symmetry, shear stresses can not develop on it. Hence OC is a principal

stress trajectory. Based on the equations of equilibrium, Jaky expressed the coefficient of earth pressure at-rest with the angle of internal friction,

$$K_o = (1 - \sin \phi) \frac{1 + \frac{2}{3} \sin \phi}{1 + \sin \phi} \quad (2.6)$$

In 1948, Jaky presented a simplified version of the expression given by Eq. 2.6.

$$K_o = 1 - \sin \phi \quad (2.7)$$

These expressions were the first attempt to relate the coefficient of earth pressure at-rest to the angle of resistance of the soil. Eq. 2.7 is still widely used due to its practical significance and attractive simplicity. It should be mentioned that Jaky's analysis was for a soil with  $\phi = \phi_{cv}$ . Thus, these expressions were suitable for  $K_o$  of sedimented, normal consolidated clays and granular materials that have not been densified by vibration or compaction.

## 2.2 Effects of Soil Compaction

Compaction of soil can produce a stiff, settlement-free and less permeable mass. It is usually accomplished by mechanical means that cause the density of soil to increase. At the same time the air voids are reduced and the co-ordination number of the grains is increased. It has been realized that the compaction of the backfill material has an important effect on the earth pressure on the wall.

Some theories introduce the idea that compaction represents a form of overconsolidation, where stresses resulting from a temporary or transient

loading condition are retained following removal of this load.

### 2.2.1 Study of Peck and Mesri

Based on the elastic analysis, Peck and Mesri (1987) presented a calculation method to evaluate the compaction-induced earth pressure. The lateral pressure profile can be determined by four conditions on  $\sigma_h$ , as illustrated in Fig. 2.4 and summarized in the following.

1. Lateral pressure resulting from the overburden of the compacted backfill,

$$\sigma_h = (1 - \sin \phi) \gamma z \quad (2.8)$$

2. Lateral pressure limited by passive failure condition,

$$\sigma_h = \tan^2(45 + \phi/2) \gamma z \quad (2.9)$$

3. Lateral pressure resulting from backfill overburden plus the residual horizontal stresses,

$$\sigma_h = (1 - \sin \phi) \gamma z + \frac{1}{4} (5^{1.2 \sin \phi} - 1) \Delta \sigma_h \quad (2.10)$$

where  $\Delta \sigma_h$  is the lateral earth pressure increase resulted from the surface compaction loading of the last backfill lift and can be determined based on the elastic solution.

4. Lateral pressure profile defined by a line which envelops the residual lateral pressures resulting from the compaction of individual backfill lifts. This line can be computed by Eq. 2.11.

$$\frac{\Delta\sigma_h}{\Delta z} = \frac{1 - \sin\phi}{4} (5 - 5^{1.2\sin\phi}) \gamma \quad (2.11)$$

Fig. 2.4 indicates that near the surface of backfill, from point a to b, the lateral pressure on the wall is subject to the passive failure condition. From b to c, the overburden and compaction-induced lateral pressure profile is determined by Eq. 2.10. From c the lateral pressure increases with depth according to Eq. 2.11 until point d is reached. Below d, the overburden pressure exceeds the peak increase in stress by compaction. In the lower part of the backfill, the lateral pressure is directly related to the effective overburden pressure.

### 2.2.2 Study of Chen

Chen (2003) utilized the NCTU model wall facility to investigate the earth pressures against a non-yielding wall with a 250 mm × 250 mm vibratory compactor. Chen (2003) represented four points of view: (1) compaction process does not result in any residual stress in the vertical direction. The effects of vibratory compaction on vertical overburden pressure are insignificantly, as indicated in Fig. 2.5; (2) after compaction, the lateral stress measured near the top of backfill is almost identical to the passive earth pressure estimated with Rankine theory (Fig. 2.6). The compaction-influenced zone rises with rising compaction surface. Below the compaction-influenced zone, the horizontal stresses converge to the earth pressure at-rest, as indicated in Fig. 2.6(e); (3) when total (static + dynamic) loading due to the vibratory compacting equipment exceeds the bearing capacity of foundation soils, the mechanism of vibratory compaction on soil can be described with the bearing capacity failure of foundation soils; and (4) the vibratory compaction on top of the backfill transmits elastic waves through soil elements continuously. For soils below the compaction-influenced zone, soil particles are vibrated. The passive state of stress among particles is disturbed.

The horizontal stresses among soil particles readjust under the application of a uniform overburden pressure and constrained lateral deformation, and eventually converge to the at-rest state of stress.

## 2.3 Methods to Estimate Lateral Pressure on Silos and Bunkers

These methods are based on equilibrium of the stored material in a static condition. Elastic interaction with the bin structure is not considered, nor is strain energy in either the stored material or the structure.

### 2.3.1 Janssen's Method

Janssen (1895) was the first to derive the differential equation for the equilibrium of a slice of solid in a silo. Janssen assumed that the ratio of horizontal pressure against the wall to the mean vertical stress in the stored solid (the lateral pressure ratio  $K$ ) is invariant with depth in the silo. Janssen's method is based on equilibrium of a thin horizontal layer of stored material, as shown in Fig. 2.7. Equating the vertical forces to zero gives:

$$qA + \gamma A dy = A \left[ q + dy \frac{dq}{dy} \right] + \mu' p (U dy) \quad (2.12)$$

where

$q$  = static vertical pressure at depth  $Y$

$A$  = area of horizontal cross section through the silo

$U$  = perimeter of horizontal cross section

$p$  = pressure of stored material against walls at depth  $Y$  below surface of stored material

$\mu' = \tan \delta =$  coefficient of friction between stored material and wall

$\gamma =$  unit weight of stored material

Substituting  $kq$  for  $p$ , and “hydraulic radius”  $R$  for  $A/U$ , the differential equation of equilibrium becomes:

$$dq/dy = \gamma - \frac{\mu'k}{R}q \quad (2.13)$$

where  $k$  is the ratio of horizontal pressure to vertical.

The solution to this differential equation is the Janssen’s formula for vertical pressure at depth  $Y$ :

$$q = \frac{\gamma R}{\mu'k} \left[ 1 - e^{-\mu'kY/R} \right] \quad (2.14)$$

Hence, to compute the horizontal pressure  $p$ , Eq. 2.14 is multiplied by  $k$ . Thus, the Janssen’s equation for horizontal pressure is:

$$p = \frac{\gamma R}{\mu'} \left[ 1 - e^{-\mu'kY/R} \right] \quad (2.15)$$

The above derivation makes no assumption as to the shape of the silo’s cross section. If the cross section is rectangular with side lengths  $a$  and  $b$ , there will have different pressures on short and long sides. A common procedure is to let  $R = a'/4$  when computing pressure on the long side  $b$ , where:

$$a' = \frac{2ab}{a+b} \quad (2.16)$$

An alternate value of  $a'$  suggested by Reimbert and Reimbert (1976) is to use



$$a' = \frac{2ab - a^2}{b} \quad (2.17)$$

Based on the Janssen's method, Fig. 2.8 estimates the distribution of earth pressure acting on the wall of a rectangular bunker filled with dry Ottawa sand. It is assumed that the rectangular storage bunker has a constant long-side length  $b = 1.5$  m, while the short-side width varies from 50 to 1500 mm. In Fig. 2.8, it is found that the horizontal earth pressure decreases with the decrease of the short-side width  $a$ . Fig. 2.8 shows that the estimation of earth pressure with Jaky's formula appears to be conservative.

### 2.3.2 Reimbert and Reimbert's Method

In 1953 and 1954, Reimbert and Reimbert presented their method for computing static pressure on the silo walls due to the stored material. Their derivation recognizes that at large depth  $Y$ , the distribution of lateral pressure becomes asymptotic to the vertical axis. This can be shown by plotting pressures given by the Janssen equation or by noting that for large  $Y$ -values, the first derivative,  $dp/dy$ , approaches zero. At that depth, the lateral pressure reaches a maximum, shown as  $p_{\max}$  on Fig. 2.9(a). A lamina of material at this depth shows in Fig. 2.9(b). Assuming it has equal vertical pressure above and below. Consequently, the lamina weight is exactly balanced by wall friction, or:

$$\gamma A dy = \mu' p_{\max} U dy \quad (2.18)$$

Thus:

$$p_{\max} = \gamma R / \mu' \quad (2.19)$$

where  $R$  is the hydraulic radius,  $A/U$ .

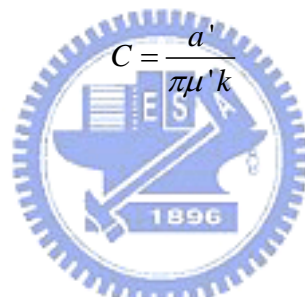
Note that, whereas the Janssen equations were derived from theory alone, the Reimbert and Reimbert's equations depend on the shape of a curve suggested by experimental data.

The Reimbert and Reimbert's equation for lateral static pressure at depth  $Y$  is:

$$p = p_{\max} \left[ 1 - \left( \frac{Y}{C} + 1 \right)^{-2} \right] \quad (2.20)$$

For rectangular silos with short-side width  $a$  and long-side length  $b$ ,  $p_{\max}$  and  $C$  (characteristic abscissa) on the longer wall are as follows:

$$p_{\max} = \gamma a' / 4\mu' \quad (2.21)$$



$$C = \frac{a'}{\pi\mu'k} \quad (2.22)$$

where  $a' = \frac{2ab - a^2}{b}$ .

Based on Reimbert and Reimbert's method, Fig. 2.10 estimates the distribution of earth pressure acting on the wall of a rectangular silo filled with dry Ottawa sand. It is assumed that the rectangular silo has a constant long-side length  $b = 1.5$  m, while the short-side width varies from 50 to 1500 mm. In Fig. 2.10, it is found that the horizontal earth pressure decreases with the decrease of the short-side silo width  $a$ . Near the top of the silo wall, estimation of horizontal pressures based on Reimbert and Reimbert's method are higher than Jaky's solution. With the decrease of short-side width  $a$ , Reimbert and Reimbert's solution will be much smaller than Jaky's solution near the bottom of walls.

### 2.3.3 Spangler and Handy's Method

Fig. 2.11 represents a section of a ditch conduit 1 unit in length. Considering a thin horizontal element of the fill material of height  $dh$  located at any depth  $h$  below the ground surface. Equating the upward and downward vertical forces on the element, the following equation is obtained.

$$V + dV + 2K\mu' \frac{V}{B_d} dh = V + \gamma B_d dh \quad (2.23)$$

where

$V$  = vertical force on the top of the element

$V + dV$  = vertical force on the bottom of the element

$\gamma B_d dh$  = weight of the fill element

$K(V/B_d)dh$  = the lateral force on each side of the element, it is assumed that the

vertical pressure on the element is uniformly distributed over the width  $B_d$ . Since the element has a tendency to move downward in relation to the sides of the ditch, these lateral pressures induce upward shearing forces equal to  $K\mu'(V/B_d)dh$ .

Eq. 2.23 is a linear differential equation, the solution for  $V$  is:

$$V = \gamma B_d^2 \frac{1 - e^{-2K\mu'(h/B_d)}}{2K\mu'} \quad (2.24)$$

Fig. 2.12 (a) shows some retaining walls are built in front of a stable rock face, not so much to retain soil as to prevent rockfalls. Granular backfill placed in the relatively narrow gap between the wall and the natural outcrop is partly supported by friction on each side, from the wall and from the outcrop. Since the friction is distributed vertically it reduces vertical stress within the soil mass, which in turn reduces the horizontal stress and the overturning moment. The weight of  $W$  of a soil prism between the wall and the rock face parallel to the wall and at a distance  $B$  from the wall (Fig. 2.12 (a)) is:

$$W = \gamma Bh \quad (2.25)$$

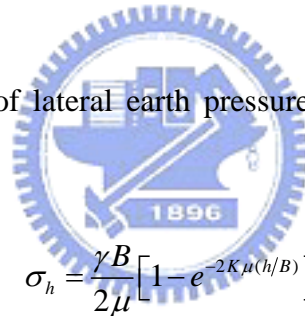
where  $\gamma$  is the unit weight of the soil, and  $h$  is the height down from the top of the wall, as shown in Fig. 2.12(a). The vertical unsupported force  $V$  from this weight is:

$$V = W - 2F \quad (2.26)$$

where  $F$  is the vertical component of wall friction. The vertical stress at any height  $h$  is  $\sigma_v = V/B$ , and the horizontal stress is:

$$\sigma_h = K \frac{V}{B} \quad (2.27)$$

where  $K$  is the coefficient of lateral earth pressure. Substitution for  $V$  from Eq. 2.24, gives:



$$\sigma_h = \frac{\gamma B}{2\mu} \left[ 1 - e^{-2K\mu(h/B)} \right] \quad (2.28)$$

where  $\mu = \tan \delta$ ,  $\mu$  is the coefficient of friction between the soil and the wall.

Some solutions of Eq. 2.28 for different values of  $B$  are shown in Fig. 2.12(b). It can be seen that the soil pressure, instead of continuing to increase with increasing values of  $h$ , level off at a maximum value defined by Eq. 2.28. When  $h$  approaches

$$\sigma_{\max} = \frac{\gamma B}{2\mu} = \frac{\gamma B}{2 \tan \delta} \quad (2.29)$$

Based on Spangler and Handy's method, Fig. 2.13 estimates the distribution of earth pressure in a narrow gap filled with dry Ottawa sand with different

distance  $B$ . For  $B = 1500$  mm, estimation of horizontal pressure with Spangler and Handy's is fair good agreement with Jaky's solution. In Fig. 2.13, it can be found that, with wall height  $H = 1.5$  m, horizontal earth pressures decrease with the decrease of distance  $B$ . It is obvious that, when the retaining wall is near to the rock face, the distribution of horizontal pressure may not be linear, and may not increase with depth.

Fig. 2.14 shows the comparison of earth pressure calculated with Janssen, Reimbert and Reimbert, and Spangler and Handy theories for the wall height  $H = 1.5$  m and the spacing between two walls  $d$  is 0.9 m. From Fig. 2.14, it can be observed that calculated Janssen's earth pressure is similar to the Rankine active pressure. Spangler and Handy's earth pressure distribution is similar to Jaky's solution. Among three solutions, Reimbert and Reinmert's prediction is the largest, while Janssen's lateral pressure is the lowest. The theoretical solutions obtained will be compared with the test results in chapter 6.

#### 2.3.4 Study of Frydman and Keissar

Frydman and Keissar (1987) used the centrifuge modeling technique to test a small model wall, and changes in pressure from the at-rest to the active condition were observed. The centrifuge system has a mean radius of 1.5 m, and can develop a maximum acceleration of 100 g, where g is acceleration due to gravity. The models are built in an aluminum box of inside dimensions 327 × 210 × 100 mm. Each model includes a retaining wall made from aluminum (195 mm high × 100 mm wide × 20 mm thick) as shown in Fig. 2.15. The rock face is modeled by a wooden block, which can, through a screw arrangement, be positioned at varying distances  $d$  from the wall. Face of the block is coated with the sand used as fill, so that the friction between the rock and the fill is equal to the angle of internal friction of the fill. Frydman and Keissar found that Spangler and Handy's solution may be used for estimating

lateral pressure for the no-movement ( $K_0$ ) condition.

